Experimental and numerical assessment of EBF structures with shear links

Silvia Caprili [a], Nicola Mussini [*] and Walter Salvatore [b]

Department of Civil and Industrial Engineering, University of Pisa, Largo Lucio Lazzarino 1, 56122 Pisa, Italy

Abstract. Eccentrically braced frames (EBF) represent an optimal structural solution for seismic prone areas, being able to provide high dissipative capacity and good elastic stiffness, to withstand strong seismic events without significant loss of bearing capacity and to avoid damage to non-structural elements in case of low and moderate earthquakes. The accurate knowledge of the cyclic behaviour of the dissipative links, characterizing the whole performance of EBFs, is required to optimize the structural properties and to refine the design techniques adopted for multi-storey buildings' analysis. Reliable numerical models for the links, at the same time requiring a limited computational effort, are then needed. The present work shows the results of a wide experimental test campaign executed on real-scale one storey/one bay frames with horizontal and vertical links, together with the elaboration of a simple semi-analytical model for the quick representation of the cyclic behaviour of shear links.

Keywords: eccentrically braced frames; experimental tests; link; numerical analyses; overstrength factor

1. Introduction

Eccentrically Braced Frames (EBF) represent the optimal solution to join the elastic stiffness of Concentrically Braced Frames (CBF) and the high ductility of Moment Resisting Frames (MRF), providing a good behaviour towards both frequent and rare seismic events requiring, respectively, the limitation of damages to non-structural elements and the dissipation of the stored seismic energy (Engelhardt and Popov 1989a, Hjelmstad and Lee 1989, Popov 1983, Roeder and Popov 1978, Kasai and Popov 1986, Richards and Uang 2005, Qi *et al*. 2017, Lian *et al*. 2015, Mohammadi and Sharghi 2014). The dissipative capacity is fully devoted to the development of high plastic deformations in correspondence of links; all the other elements and components – including connections – are designed to remain in the elastic field, avoiding the damages observed in the case of buildings designed before the introduction of the Performance Based Design approach (Bertero *et al*. 1994, Nakashima 1998, Nakashima and Bruneau 1995).

Current design codes (Eurocode 8 - EN 1998-1:2005 2005, D.M.14/01/2008 2008, FEMA 356 2000) consequently introduce the *overstrength factor* (Ω) to achieve a desired 'global/ductile' collapse mechanism, defined as the ratio between the plastic design strength of the dissipative element and the resulting seismic action. Several studies in the current scientific literature (Badalassi *et al*. 2013, Braconi *et al*. 2015, Badalassi *et al*. 2017, Bosco and Rossi 2009, Bruneau *et al*. 2011) highlighted, on the contrary, the

general overestimation of Ω factors and, besides, the global oversizing of the non-dissipative elements due to second order effects, buckling limitations and vertical actions, resulting in a non-optimized design. D'Aniello *et al*. (2012) proposed a new approach for the estimation of the over-strength factor of shear links, limiting the resulting indications to elements of specific length, expressed as function of the ratio between the flexural and the shear capacity.

The reliable representation of the cyclic/seismic behaviour of links is, however, needed to investigate the global structural performance of EBF buildings and to analyse the efficiency of current standards in the protection of the non-dissipative members and in the optimization of the ductile behaviour of proposed structures (Bosco *et al*. 2015). Performing reliable numerical analyses can help the investigation of the structural buildings' behaviour and the following definition of generalized and efficient design rules. The accuracy of results depends on the correct modelling of the links, including their flexural/shear behaviour, especially in the post-elastic field. The results of several experimental tests' campaigns discussed in the current and past scientific literature (Engelhardt and Popov 1989b, Hjelmstad and Popov 1983, Okazaki and Engelhardt 2007) constitute the base for the the development of different modelling approaches used to represent the structural performance of EBF frames and components, including connections.

Nonlinear modelling techniques, spreading from concentrated plasticity models to distributed fibre elements and, finally, to complex continuum models (D'Aniello *et al*. 2012) shall be properly defined depending on the purpose of the analysis, being their accuracy strongly dependent on the computational burden and on the information that wants to be achieved. Gilberson (1969) elaborated a one component model with concentrated plastic hinges at the

---

[*] Corresponding author, Ph.D.,
  E-mail: nicola.mussini@ing.unipi.it
[a] Assistant Professor
[b] Full Professor

two ends, Rides and Popov (1993) calibrated a two-components model constituted by beams working in parallel, Lignos and Krawinkler (2011) proposed a multi-linear plastic spring model describing both the monotonic and the cyclic behaviour of I-shaped section steel beams, accounting for strength deterioration due to material damage and local buckling phenomena, applicable to long/bending links.

With the aim of investigating the influence of material variability on the ductile behaviour of EBF structures, Braconi *et al*. (2015) and Badalassi *et al*. (2013, 2017) adopted a simple model for links with steel or steel/concrete composite structure using a bilinear constitutive relationship to account for the shear behaviour; this simplification was accepted in relation to the main aim of the work, where hundreds of simulations were executed to statistical research aims. Ricles and Popov (1987) and Ramadan and Ghobarah (1995) calibrated a multilinear constitutive law representing the cyclic behaviour of short/shear links; the model was later upgraded by Bouwkamp *et al*. (2016), introducing a multilinear plastic spring element working in shear with strain hardening law defined according to Mróz (1969). Richards (2010) proposed a model for EBF structures able to take into account, in the estimation of the horizontal displacement of EBFs, the deformation contributions of braces, beams (axial and flexural) and link in shear. Mohammadi and Sharghi (2014) elaborated a multi-spring model with stiffness values optimized for nonlinear time histories analyses, valid alternative to reduce the computational burden typical of refined solid models. Recently, Bosco *et al*. (2015) proposed a model for the representation of link elements, consisting in an elastic beam with plastic shear and flexural hinges located at the two ends, allowing a gradual variation of the flexural and shear stiffness of the link and including both kinematic and isotropic hardening.

Stating what above presented, whether if the dissipative behaviour of long links, governed by flexural stresses, can be easily represented through the reliable constitutive models for beam elements (Dimakogianni *et al*. 2015), the case of short/shear links is more complicated. Rides and Popov (1993), Mastrandrea and Piluso (2009) and, more recently, Ashtari and Erfani (2016) highlighted the importance of an accurate modelling of links to obtain reliable numerical outcomes both in the case of short/shear and long/bending links: despite the different dissipative mechanism, flexural forces combined with shear ones always develop, and models shall be able to reproduce both the two effects in the elastic and post-elastic fields. If the constitutive law of material is accurately calibrated, solid finite-element models, such as, for example, in the cases presented by Prinz and Richards (2009), Berman and Bruneau (2007, 2008) and others, can allow the achievement of reliable results in the description of the damage and deterioration behaviour of the dissipative elements. On the other hand, the strong numerical effort limits their possible application to the case of nonlinear dynamic analyses of multi-storey buildings, in which the reliability of results shall be necessarily related to the time requiring and computational burden (Bosco *et al*. 2015).

Basing on the previous considerations, the present paper shows the results of an experimental test campaign executed on real scale EBF specimens to investigate the structural performance of dissipative shear link elements under different cyclic loading conditions. Experimental tests were performed in the main framework of the European research project MATCH "*Material choice for seismic resistant structures (2013-2016)*", devoted to the analysis of the influence of material properties (toughness mainly) on the ductile performance of steel structures in seismic areas.

Considering the previous problems related to the modelling approach, a simple semi-analytical model for the representation of the dissipative behaviour of link elements working in shear, calibrated on the base of experimental tests' results, is then proposed. The model aims at providing a useful tool for the execution of nonlinear analyses in multi-storey EBF buildings with a reduced computational burden, including the two isotropic and kinematic hardening contributions to correctly reproduce the real experimental behaviour of link elements working in shear.

2. Experimental behaviour of EBF structures

2.1 Design of the specimens

One storey/one bay EBF real-scale prototypes with horizontal and vertical links were designed, realized and tested at the laboratory of Pisa University.

The global size of the prototypes was fixed accounting for the geometrical configurations of typical multi-storey office buildings and the available laboratory facilities. To have a preliminary idea of the shape and size of the frames, the case study buildings designed in a past research project (Badalassi *et al*. 2013) were considered.

The EBF prototypes have a span length equal to 5.0 m and a storey height up to 3.0 m; two different configurations – one with vertical link and the other one with horizontal link – were studied. In both cases, short shear links were adopted; steel grade S355 was used for all the elements. The design of the frames was executed in compliance with current seismic design regulations (Eurocode 8 - EN 1998-1:2005 2005, D.M. 14/01/2008 2008); elements' sections were optimized pursuing easiness in joints and connections and concentrating the whole deformation in dissipative elements. This design choice allowed to easy replace links after damages, following the same approach adopted in the tests' campaign presented by Manfredi *et al*. (2015).

The preliminary design of links was performed through a limit analysis assuming a rigid behaviour of the whole frame and deformations concentrated in correspondence of links. A limit angular rotation equal to 110 mrad was adopted for the links: this value, in agreement with FEMA 356 prescriptions, is higher than the one foreseen by Eurocode 8 (80 mrad) but reliable in relation to what observed during experimental tests, revealing a global higher rotational capacity and higher over-strength factors (Keith and Egor 1983, Peter *et al*. 2010, Mazzolani *et al*. 2009). A safety factor equal to 1.30 was also applied.

The minimum horizontal force F_h and displacement δ_h

required to achieve the full plastic behaviour of EBFs adopted in the design are summarized by Eqs. (1) and (2), being $V_{u,link}$ equal to 1.5 times the shear force at the elastic limit of the link $V_{y,link}$, B and H respectively the geometric span length and height, e the length of the link and γ the angular distortion of the link, according to Fig. 1.

$$
\begin{aligned}
F_h &= V_{u,link} \cdot \frac{B}{2H} \quad \text{horizontal link} \\
F_h &= V_{u,link} \quad \text{vertical link}
\end{aligned}
\tag{1}
$$

$$
\begin{aligned}
\delta_h &= \frac{\gamma \cdot e}{B - e} H \quad \text{horizontal link} \\
\delta_h &= \gamma \cdot e \quad \text{vertical link}
\end{aligned}
\tag{2}
$$

Basing on these assumptions, HEA100 profiles with length equal to 300 mm for the horizontal link and HEB120 profiles of length equal to 150 mm for the vertical link were selected. Table 1 summarizes the expected horizontal forces and displacements obtained using the Eqs. (1) and (2) for links in the two different configurations (the subscript "*y*" refers to the first yielding condition).

The design of non-dissipative elements followed the EN 1998-1:2005 approach through the use of Eq. (3), being $F_{h,y}$ the horizontal force used to yield the link, Ω the design over-strength factor of the dissipative element and γ_{ov} the material overstrength factor, equal to 1.25. The ratio

$V_{y,link}/V_{Ed}$ was assumed unitary considering the achievement of the complete plastic deformation of the link during the tests; eventual higher over-strength was accounted for assuming Ω factors equal to 2.0.

$$
\Omega = 1.5 \cdot V_{y,link} / V_{Ed}
\tag{3}
$$

For both the two configurations, columns and beams were realized using HEB180 sections; for braces 2UPN160, coupled with 3 bolted connections equally spaced, were employed. Web stiffeners, equally spaced, in correspondence of horizontal links to avoid buckling phenomena of the web in the plastic field were use following EN1998-1:2005 prescriptions; no stiffeners were introduced for vertical links.

A lot of attention was paid to the design of joints and connections, aiming to simplify the replacement of dissipative elements after the damage due to the execution of experimental tests, speeding up the laboratory activities. All the connections were designed to work in friction adopting a safety factor equal to 1.50. Before realizing the connections of the real-scale specimens tested, preliminary numerical simulations were executed to evaluate the representativeness of the adopted restraints. In particular, numerical analyses were executed on the one storey/one
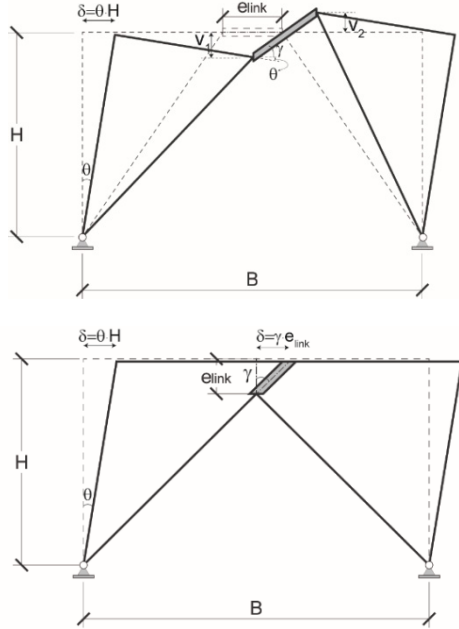

Fig. 1 Plastic deformation expected for EBF systems

Table 1 Expected forces and displacements for links

Link	e [mm]	$F_{h,y}$ [kN]	$F_{h,max}$ [kN]	$\delta_{h,y}$ [mm]	$\delta_{h,max}$ [mm] (110 mrad)
HEA100 (hor.)	300	90.1	162.3	0.8	24.0
HEB120 (vert.)	150	145.2	217.8	0.4	19.5

Table 2 Results of preliminary simulations on EBF frames with different typologies of connections

Vertical pinned braces (one fixed/one pinned connection system – finally adopted)			
	N [kN]	V [kN]	M [kN]
Beams	±72.6	±5.8	±10.9
Braces	±112.5	0.00	0.00
Columns	±4.36	0.00	0.00
Link	0.00	145.2	-21.78
Vertical fixed braces (fixed/fixed connection system)			
	N [kN]	V [kN]	M [kN]
Beams	±72.60	±2.90	±6.53
Braces	±113.98	±1.45	±4.36
Columns	±2.90	0.00	0.00
Link	0.00	145.20	-13.07 (+8.71)

Table 3 Main dimensions of the EBF specimens' elements

EBF	Vertical link	Horizontal link
Columns	HEB 180	HEB 180
Beams	HEB 180	HEB 180
Braces	2UPN 160	2UPN 160
Links	HEB 120	HEA 100
e_{Link} [mm]	150	300
H_{col} [mm]	3000	3000
L [mm]	5000	5000

bay frame with vertical link investigating the differences on resulting actions on the dissipative elements and on braces adopting a 'one pinned/one fixed connection system' and, otherwise, a 'fixed/fixed connection system'. Differences in results were negligible (Table 2), allowing the assumption of connections respectively fixed (with the beam) and pinned (with braces), making easier the replacement of the element after damage without working on the other components.

Table 3 summarizes the profiles and the main dimensions of the specimens used for the experimental tests. Figs. 2 and 3 show the final configuration of the EBFs systems with horizontal and vertical links.

2.2 Experimental test setup

Fig. 5 provides a general overview of the test set up used at the Laboratory of the University of Pisa for the EBF specimens. To avoid possible out-of-plane and buckling phenomena (global instability of the tested frames, buckling of the top beam), additional components were used to connect the EBF systems to the bidirectional concrete slab floor of the Laboratory.
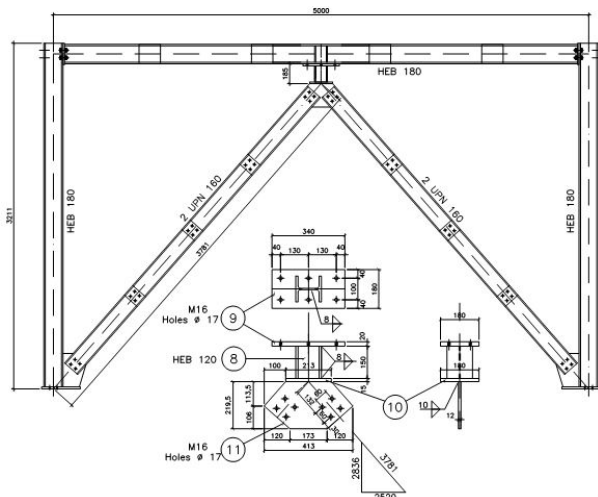

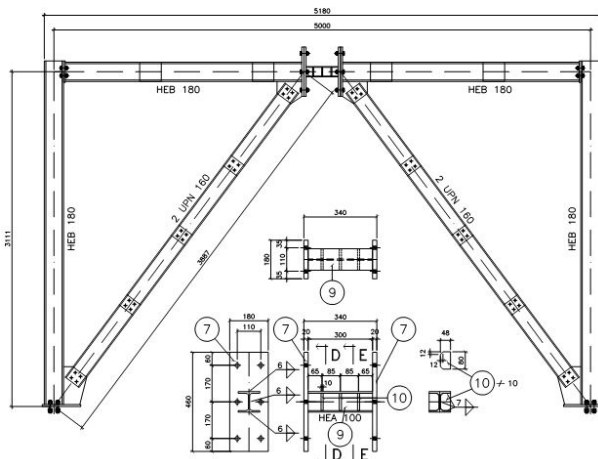Fig. 2 EBF prototypes with vertical link, details

Fig. 3 EBF prototypes with horizontal link, details

Four additional structures/substructures were adopted:

- A *rigid basement* connecting the testing prototypes to the slab of the Laboratory.
- A *stabilizing frame* avoiding the warping of the columns.
- A *loading transfer frame* connecting the EBF to the hydraulic jackets and avoiding buckling phenomena of the top beam and the whole frame.
- A *contrast frame*, to which the actuators are fixed.

The load was applied at the height of the top beam (~3.0 m) using two hydraulic jackets with maximum stroke equal to ± 150 mm and maximum load capacity equal to ± 200 kN each one, introducing a cyclic loading history. The applied load was controlled using two load cells placed between the hydraulic jackets and the loading transfer frame (Fig. 4).

The monitoring system was planned to guarantee a suitable amount of recorded information (i.e., applied force, deformation, global and local displacements). Sensors were placed to monitor the shear force-displacement behaviour of the links (or the shear - angular deformation one).

Triaxial strain gauges were applied on the link web to assess the evolution of the plastic deformation due to the shear force within the whole web of the dissipative links. Uniaxial strain gauges were placed on the top and bottom flanges at both ends of the link, to check whether a flexural mechanism can be triggered when elevated angular rotations are reached. Fig. 6 provides a schematic overview of the sensors' disposition. LVDTs were organized to account for the possible slip due to hole-to-bolt clearances. One LVDT on the actuator and one on the top beam were
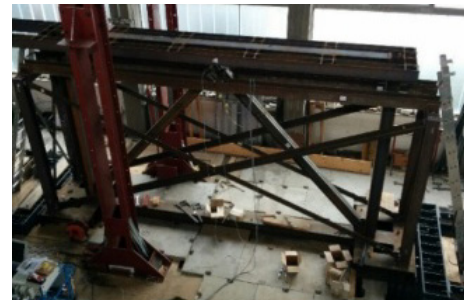

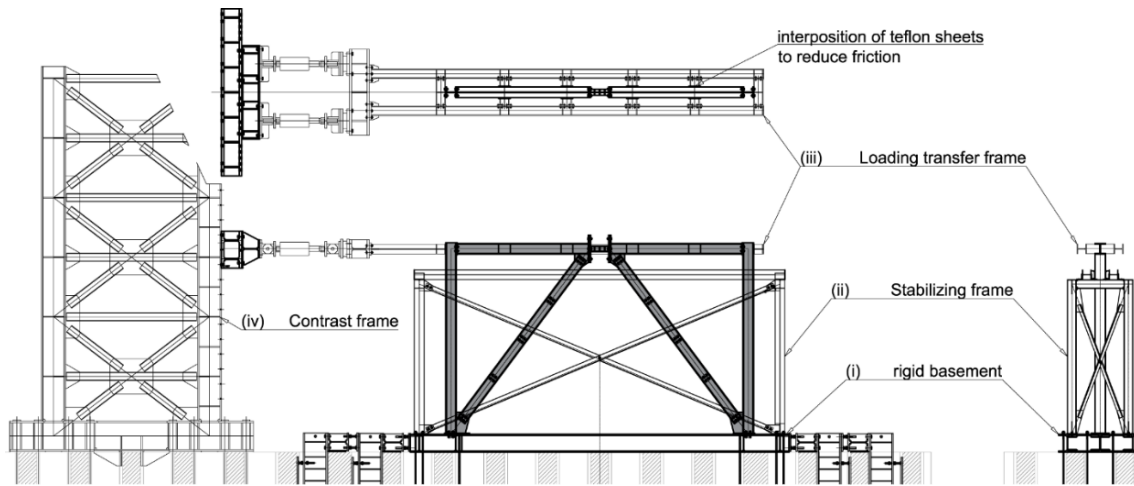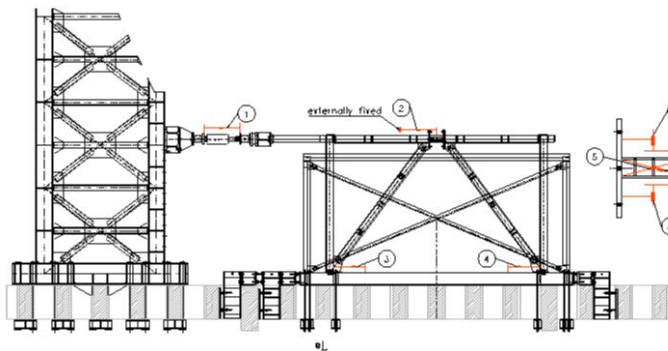Fig. 4 Assembled EBF and setup of the test in the lab

Fig. 5 General overview of the test setup used for the EBF specimens in the laboratory of Pisa University

EBF with horizontal link

LVDT1: displacement of the actuator.
LVDT2: displacement of the top beam.
LVDT3-4: relative displacement at the basement connection.
LVDT5-6: displacement of the diagonals of the link.
LVDT7-8: transversal displacement of the link.
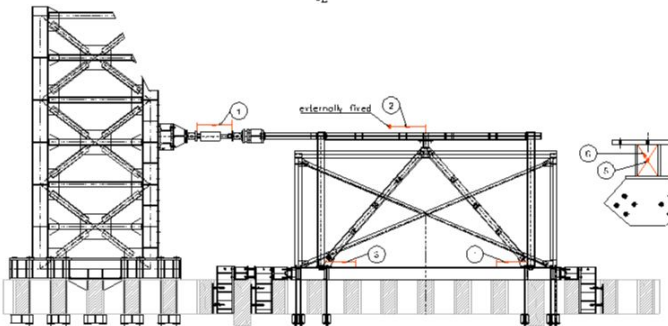
EBF with vertical link

LVDT1: displacement of the actuator.
LVDT2: displacement of the top beam.
LVDT3-4: relative displacement at the basement connection.
LVDT5-6: displacement of the diagonals of the link.
LVDT7: transversal displacement of the link.

Fig. 6 Scheme of LVDT disposition for EBF prototypes with horizontal and vertical link

(a)

(b)

Fig. 7 LVDT disposition on (a) vertical; and (b) horizontal links

Table 4 Summary of experimental tests executed

EBF Link	ECCS45 protocol		Constant amplitude	
	n°tests	e_y	n°tests	amplitude
Vertical	2	0.6 mm	1	±16.9 mm
Horizontal	2	0.8 mm	1	±21.5 mm

used to monitor the global displacement.

With reference to Fig. 7, the displacement of the link due to shear deformation, depurated from eventual slip, was evaluated monitoring the transversal deformation and the displacement of the diagonal through Eq. (4)

$$\gamma = tg^{-1} \cdot \left[\sqrt{h_i^2 + L_i^2} \cdot \frac{\Delta U_{LVDT,1} + \Delta U_{LVDT,2}}{2 \cdot (h_i + L_i)} \right] \qquad (4)$$

being $\Delta U_{LVDT,1}$ and $\Delta U_{LVDT,2}$ the relative displacement measured in correspondence of the two LVDT instruments placed along the two diagonals of the link, L_i and h_i the length and the height of the shear panel of the link.

2.3 Selection of the loading protocol

Two different loading protocols were adopted for the execution of the cyclic tests: the first one characterized by constant amplitude and the second one following ECCS45.

The application of ECCS45 loading history required the determination of the displacement e_y corresponding to yielding, evaluated adopting the simplified formulation provided by Eq. (1). The amplitude of the cyclic constant amplitude test was then imposed equal to the 85% of the displacement causing the crack initiation in the link during the application of the ECCS45 protocol.

The displacement increment e_y adopted for the ECCS45 protocol was fixed equal to 0.6 mm for the vertical link, and 0.8 mm for the horizontal one. The constant displacement amplitude (constant amplitude protocol) was set equal to ±16.9 mm and ±21.5 mm respectively in the case of vertical and horizontal links. Two tests following ECCS45 protocol and one constant amplitude test were executed for each EBF configuration; Table 4 summarizes experimental tests' parameters adopted.
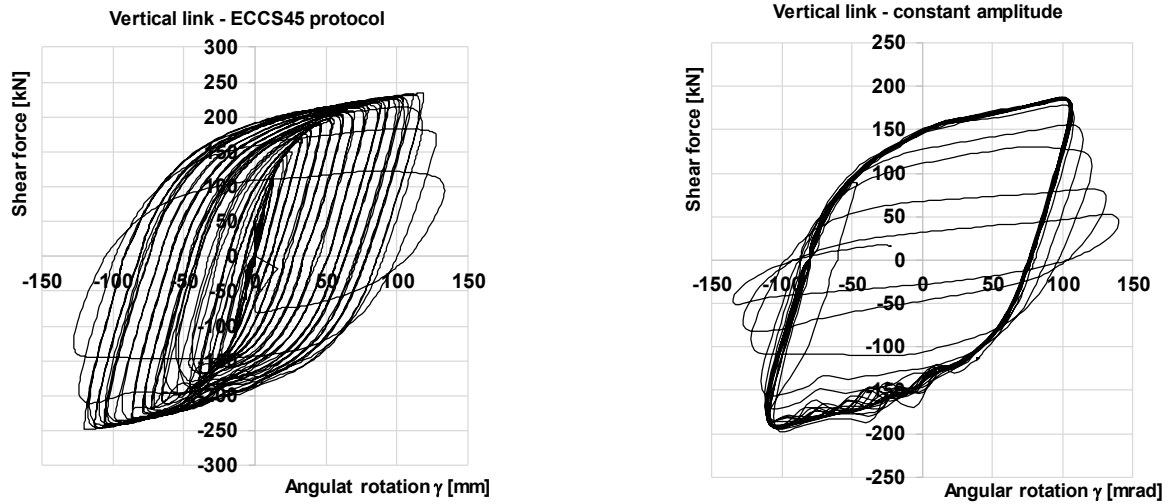

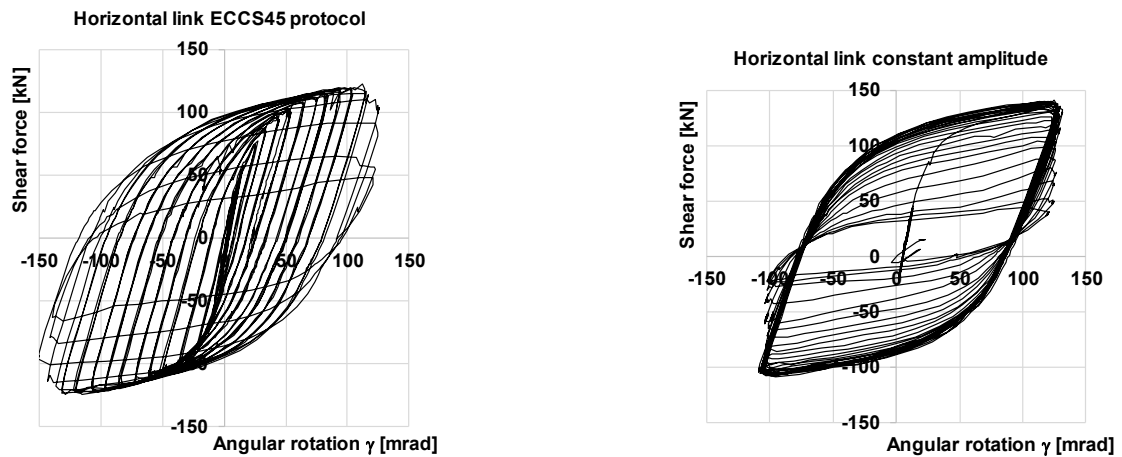Fig. 8 *F-γ* diagrams for the vertical link tested with ECCS45 and constant amplitude protocol

Fig. 9 *F-γ* diagrams for the horizontal link tested with ECCS45 and constant amplitude protocol

2.4 Experimental tests' results

2.4.1 V-γ behaviour of link elements

The typical stable hysteretic behaviour of EBF frames, as presented for example in Bruneau *et al.* (2011), was evidenced during the cyclic loading application. Figs. 8 and 9 show the experimental shear/angular distortion behaviour respectively in the case of vertical and horizontal links for ECCS45 and constant amplitude loading protocols.

Both the vertical and the horizontal links evidenced a yielding force close to the analytical design value, respectively equal to about 90 and 145 kN (Table 1), corresponding to values of yielding strength about equal to nominal ones (~355 MPa, as confirmed by tensile tests performed on dog-bone specimens extracted from the web and from the flanges of link profiles).

All the specimens experienced a crack within the web propagating parallel to the flanges, as represented in Figs.

10 and 11, respectively in the case of vertical and horizontal links. As clearly visible from the diagrams, a rather steep loss of shear capacity was observed in the case of ECCS45 protocol; in the case of constant amplitude test, the decrease of the bearing capacity was lower, resulting in a higher number of cycles up to failure.

In the case of EBF prototypes with horizontal links, the presence of equally spaced stiffeners within the web hindered the propagation of the crack. Following ECCS45, the specimens reached an average angular rotation γ close to 125 mrad (Table 5), higher than the imposed collapse limitation defined by EN1998-1:2005 and FEMA 356, respectively equal to 80 and 110 mrad. In the case of constant amplitude tests, crack initiation was observed at the 24th cycle.

In the case of EBF prototypes equipped with vertical links, the ECCS45 tests resulted in an average ultimate angular rotation equal to 122 mrad while, following the constant amplitude protocol, collapse was achieved in correspondence of the 22nd cycles. Table 5 summarizes the results of tests when collapse occurred.

The plastic branch of the experimental curves obtained with ECCS45 loading protocol can be subdivided in two parts: the first one, between the yielding point and the achievement of 110 mrad of angular rotation, was characterized by a mixed isotropic and nonlinear kinematic hardening (Lemaitre and Chaboche 1994) while the second branch, from 110 mrad up to the crack propagation, was governed by a sub-horizontal branch, evidencing that both the isotropic hardening and nonlinear hardening are saturated.

Table 5 Results of the experimental tests

Vertical link	Test 1 ECCS	Test 2 ECCS	Test 3 const. ampl.	Design values
γ_{ult} [mrad]	125	119	110	110
F_{max} [kN]	244.0	248.7	245.7	217.8
Horizontal link	Test 1 ECCS	Test 2 ECCS	Test 3 const. ampl.	Design values
γ_{ult} [mrad]	128	123	110	110
F_{max} [kN]	172.6	175.9	166.7	162.3

(a)   (b)   (c)

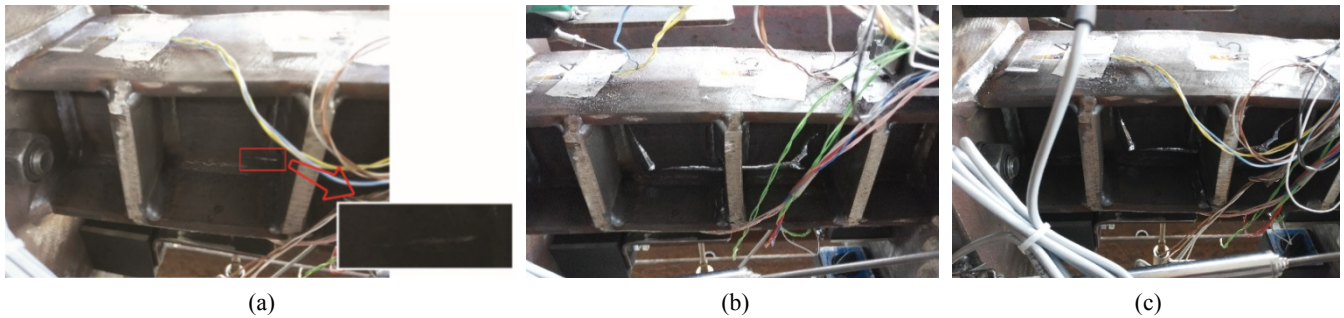Fig. 10 Horizontal links: (a) web crack initiation; (b)-(c) web crack propagation (test 1 ECCS a and test 3 ECCS)
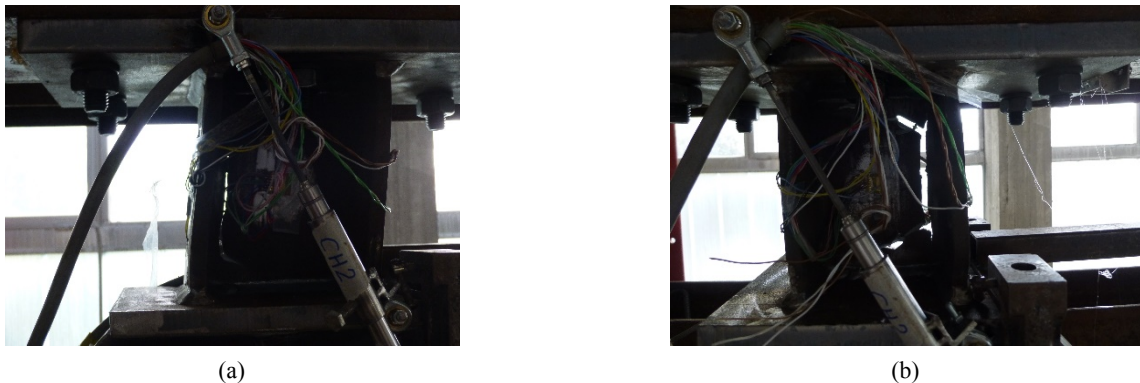

(a)   (b)

Fig. 11 Damage mechanism in the vertical links: web crack propagation (test 1 ECCS a and test 3 ECCS)
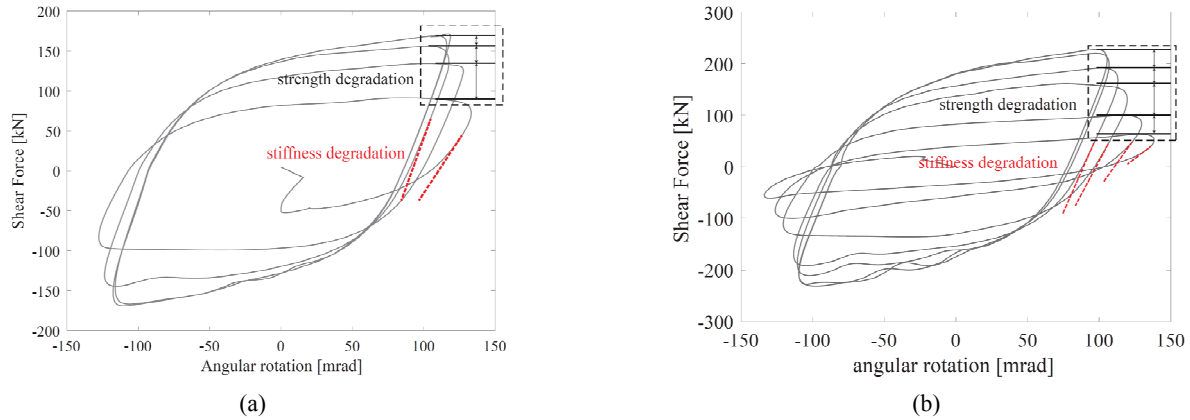
(a)

(b)

Fig. 12 Degrading behaviour after the crack initiation: a) ECCS45 – horizontal link; b) constant amplitude – vertical link

The cyclic behaviour of the vertical and horizontal links was stable until crack initiation occurred in correspondence of the web (Figs. 10-11): from that point on, the link evidenced a degrading behaviour in terms of strength and stiffness. The stiffness degradation was clearly recognizable analysing the post-critical behaviour of the experimental tests (Fig. 12) performed with the constant amplitude protocol. In general, once the crack started to propagate, the maximum shear force that the web of the link could withstand progressively reduced from one cycle to the next.

Thereby, when the crack propagated, the web was progressively unloaded and the bearing capacity of the links resulted governed only by the flexural behaviour provided by the flanges, evidencing a reduced load bearing capacity and lower elastic stiffness as well.

2.4.2 Evaluation of Ω factors

To assess the efficiency of the capacity design approach in the determination of elements' sections, overstrength factors of dissipative links were evaluated from the experimental tests. The '*observed*' experimental over-strength factor Ω_{obs} was defined following Equation (5)

$$\Omega_{obs} = \frac{V_{u,link}}{V_{y,link}} \quad (5)$$

being $V_{u,link}$ the shear associated to the collapse of the element and the $V_{y,link}$ the shear value that yields the element itself, defined according to what already presented in Table 1.

Considering the vertical link, for an angular rotation equal to 80 mrad, the observed over-strength factor was in good agreement with Eurocode 8 prescriptions, being equal to 1.56 (i.e., 13% higher than standard value, Table 6). Higher differences were observed at the collapse (average value equal to 118 mrad, Table 5), with values up to 1.68. Similar considerations were executed in the case of the horizontal link, with discrepancies higher than the 30% respect to Eurocode 8 limitations and Ω factors close to 1.90 at 80 mrad and 2.10 at collapse.

What above presented highlighted the general oversizing of dissipative structural elements of EBFs designed according to the capacity design approach

Table 6 Ω factors evaluated from experimental tests

Protocol	Ω at collapse	Ω at 80 mrad	Ω at 110 mrad
ECCS 1	1.68	1.56	1.67
ECCS 2	1.71	1.58	1.69
Const. ampl.	1.67	-	-
Protocol	Ω at collapse	Ω at 80 mrad	Ω at 110 mrad
ECCS 1	2.1	1.87	2.02
ECCS 2	2.15	1.92	2.01
Const. ampl.	2.04	-	-

imposed by EN1998-1:2005, that is, otherwise, more relevant in the case of frames equipped with horizontal links.

3. Numerical modelling of EBF structures

To represent the structural performance of EBF structures and the contribution of link elements, a semi-analytical model, calibrated basing on experimental tests' results, was then proposed. The semi-analytical model provides reliable results together with a reduced computational effort, representing a valid and useful tool for the execution of complex multi-storey buildings' analysis, alternative to what presented in the current scientific literature.

Background and motivations

As highlighted, the reliability of numerical analyses is strictly affected by the accuracy of the adopted models, that is, at the same time, associated to the computational burden and time requiring. In relation to the aims of the simulations (e.g., parametric studies, statistical analyses, etc.) the most appropriate modelling strategy shall be selected.

In Braconi *et al.* (2015), for example, a bilinear constitutive shear/angular distortion law was adopted for the modelling of links in EBFs with the aim of investigating the influence of material properties variability through the elaboration of fragility curves. This approach allowed to execute numbers of Incremental Dynamic Analyses (IDA) with several time histories and for lots of representative

case studies within relatively reduced computational times. Prinz and Richards (2009), aiming at analysing the possibility to adopt reduced web sections for EBFs, realized an Abaqus finite-element solid model using solid elements for the link and column flanges in the connection regions, with opportunely studied restraints to transfer forces. Models like this well describe the behaviour of dissipative components but require a strong effort in both modelling and analysis.

Several discrepancies can be observed using different modelling techniques: Fig. 13 shows the comparison of results obtained adopting three different modelling strategies for the dissipative element of a benchmark structure consisting in a one storey/one bay EBF equipped with vertical shear link. The benchmark presented link profile HEB120 of length equal to 150 mm, columns and beams HEB180 and braces realized with 2UPN160, height of the columns equal to 3000 mm and span length up to 5000 mm. All profiles were realized using steel grade S355. Three different approaches were adopted:
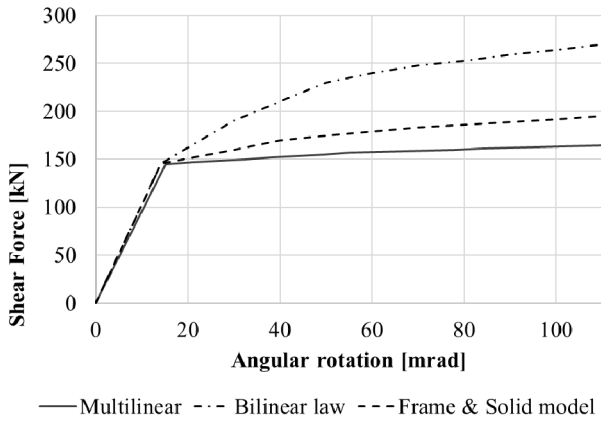

Fig. 13 Comparison of results on the EBF benchmark

(1) A "*Bilinear-law model*" following the what already applied in Badalassi *et al*. (2013, 2017) and Braconi *et al*. (2015), with fibre sections, elastic shear relationship for non-dissipative components and bilinear constitutive shear/distortion law for dissipative links.

(2) A "*Frame & Solid model*" in which the frame was modelled with elastic beam elements while a solid element with a kinematic hardening rule was adopted for the dissipative shear link.

(3) A "*Multilinear model*", following the formulation proposed by Ricles and Popov (1987), with a multilinear plastic spring with shear and flexural behaviour for the dissipative elements.

The parameters adopted for the three models are summarized in Table 7. Fig. 13 shows the comparison of the shear/distortion curves obtained subjecting the EBF one storey/one bay frame to a pushover analysis with increasing monotonic load applied in correspondence of the top storey.

The "*Bilinear-law model*" (Badalassi *et al*. 2013, 2017, Braconi *et al*. 2015), despite its simplicity and the reduced associated computational effort, overestimated the stiffness in the post-elastic field showing a more rigid behaviour respect to other solutions. This was evident when the plastic mechanism was governed by the shear and in presence of large displacements, due to the decomposition of the shear force into two contributions including a tensile force generating the increase of the elements' stiffness (Fig. 1).

The "*Frame & Solid model*" was able to represent the evolution of the plastic deformation within the web; a fine calibrated material, accounting for the strain hardening and isotropic hardening, strongly influencing the cyclic behaviour of the material, was needed.

This condition leaded to a high computational and modelling effort especially when such model was applied to multi-storey buildings, otherwise representing ordinary constructions.

Table 7 Parameters adopted for the modelling

Bilinear-law model (Badalassi *et al*. 2013)	$V_{y,link}$	$V_{u,link}$	K_{link}	$D_{y,link}$	$D_{u,link}$
	$\dfrac{f_y}{\sqrt{3}} \cdot A_v$	$\dfrac{f_u}{\sqrt{3}} \cdot A_v$	$\dfrac{G \cdot A_v}{e}$	$\dfrac{V_y}{K_{shear}}$	$\gamma_u \cdot e$
Frame & Solid model	f_y [MPa]	f_u [MPa]	True-stress	True-strain	
	$\dfrac{f_y}{\sqrt{3}} \cdot A_v$	$\dfrac{f_u}{\sqrt{3}} \cdot A_v$	$\dfrac{G \cdot A_v}{e}$	$\dfrac{V_y}{K_{shear}}$	
Multilinear model (Ricles and Popov 1987)	1st branch	2nd branch	3rd branch	4th branch	Ultimate d_u
	$K_1 = \dfrac{G \cdot A_v}{e_{link}}$ $V_1 = \dfrac{f_y \cdot A_v}{\sqrt{3}}$	$K_2 = 0.03 \cdot K_1$ $V_2 = 1.26 \cdot V_1$	$K_3 = 0.015 \cdot K_1$ $V_3 = 1.40 \cdot V_1$	$K_4 = 0.002 \cdot K_1$	$\gamma_u \cdot e$

The effort required for the calibration of the "*Multilinear model*" depended upon the number of subdivisions of the backbone curve. According to Ricles and Popov (1987), for example, the backbone curve was subdivided in 4 segments, requiring at least 2 parameters for each segment. In particular, referring to Table 7, the first branch, representing the elastic branch of the curve, was directly obtained by means of analytical relations providing the elastic stiffness and the yielding force; the other three branches were defined knowing the slope of the segment and the upper limit force. Adopting the values proposed by the authors and comparing results with the other two modelling solutions, the multilinear model underestimated the plastic branch. Thereby, the calibration of additional several parameters was required to achieve a reliable solution coherent with the results of the solid model.

What above presented highlights the need of reliable and simple models able to quickly represent the dissipative performance of EBF structures especially in the case of multi-storey buildings, where the computational burden need necessarily to be reduced.

Proposal for a semi-analytical model for links

A semi-analytical model able to predict the post-elastic behaviour of shear links and easily adopted for the execution of nonlinear numerical analyses of multi-storey EBF buildings is then proposed.

The model consists of two flexural and shear nonlinear springs linked to work in parallel, respectively representing the shear/displacement (V-δ) and the bending/rotation (M-θ) behaviour. The scheme of the proposed model is provided by Fig. 15. Such approach, rather easy to be implemented in a finite element software, is able to avoid the drawbacks observed with the Badalassi *et al.* (2013) model as presented in the previous paragraph.
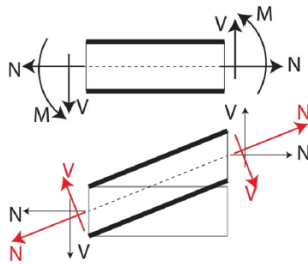

Fig. 14 Decomposition of shear force in tensile force for large displacements (*Bilinear-law model*)
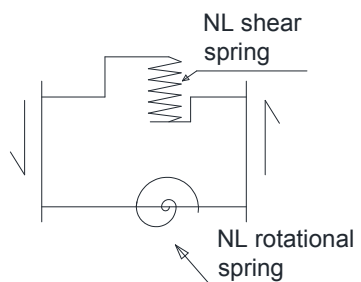

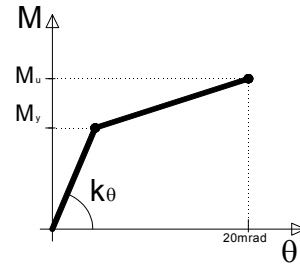Fig. 15 Scheme of the proposed model for shear links

Fig. 16 Modelling of the bending-rotation behaviour

Modelling of the bending-rotation behaviour

The M-θ relationship of the link is represented through a bilinear kinematic hardening constitutive law, whose parameters are defined through the following equations and simply represented in Fig. 16.

$$k_\theta = \frac{\beta \cdot EJ}{e_{link}} \qquad \text{initial stiffness}$$
$$M_y = (h - t_f) \cdot b \cdot t_f \quad \text{yielding moment} \qquad (6)$$
$$M_u = 1.2 \cdot M_y \qquad \text{ultimate moment (20 mrad)}$$

Being h the height of the section, b and t_f the width and the thickness of the flanges, e_{link} the length of the link and β a factor depending on the ends restraints. Considering that the vertical link elastic behaviour can be represented by a beam element with the ends pinned and fixed, β is equal to 3; for the horizontal link, belonging to a symmetric EBF configuration, β is equal to 6, since its elastic behaviour can be represented as a beam with both ends fixed.

Modelling of the shear-distortion behaviour

For the modelling of the V-γ behaviour, different constitutive laws can be adopted. In the present work, two possibilities were preliminarily investigated: the *Linear Kinematic Hardening* (LKH), frequently used to represent the nonlinear behaviour of shear links (Badalassi *et al.* 2013) and the *Non Linear Kinematic Hardening* (NLKH), accounting for both the nonlinear kinematic and isotropic hardening.

The LKH law required the determination of only three parameters: the initial stiffness (K_{ini}), the yielding force ($V_{y,link}$) and the tangent modulus of the plastic range (K_{pl}). The first two parameters were defined through analytical considerations, basing for example on what already proposed by Badalassi *et al.* (2013). The third parameter (K_{pl}) was directly dependent on the ultimate condition of the link, and was tuned considering two different situations:

(1) Ultimate strength $V_{u,link}=1.5V_{y,link}$ achieved for γ equal to 80 mrad according to Eurocode 8 (EN1998-1:2005) provisions (LKH1).
(2) Real ultimate strength (V_u) and maximum shear deformation (γ_u) defined according to experimental results, usually higher than what commonly proposed by standards (LKH2).

The NLKH law, besides the three aforementioned parameters (K_{ini}, $V_{y,link}$ and K_{pl}), required the calibration of

Table 8 Parameters for the calibration of the NLKH law

Kinematic hardening (Menegotto-Pinto law)	b_k	Hardening ratio
	R_0	
	r_1	Control the exponential transition from linear elastic to hardening asymptote
	r_2	
Isotropic hardening	b_i	Initial hardening ratio, expressed as ratio of the initial stiffness E_0 (E_i/E_0)
	b_l	Saturated hardening ratio, expressed as ratio of the initial stiffness E_0 (E_{is}/E_0)
	ρ_i	Specifies the position of the intersection point between initial and saturated hardening asymptotes
	R_i	Control the exponential transition from initial to saturated asymptote
	l_{yp}	Length of the yield plateau
Ultimate strength	R_u	Ultimate strength
	f_u	Control the exponential transition from kinematic hardening to perfectly plastic asymptote
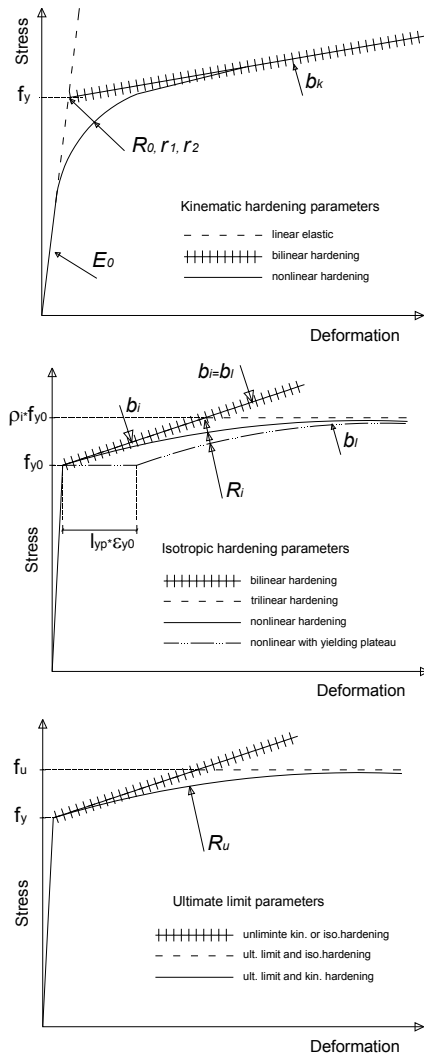
Fig. 17 Graphical interpretation of the parameters for the calibration of the NLKH law (Mazzoni *et al.* 2006)

additional parameters. In the present work, OpenSees software was adopted (Mazzoni *et al.* 2006); the NLKH law is then already implemented through the *Steel04* material model, requiring four additional parameters to define the kinematic hardening, five for the isotropic hardening, and information about the ultimate strength limit at which the isotropic behaviour is saturated (that means when only the kinematic hardening with yield plateau continues). Obviously, other software can be adopted, with opportunely calibrated parameters.

The parameters listed in Table 8 are required; their graphical interpretation is provided by Fig. 17. Referring to the kinematic hardening parameters, K_{ini}, $V_{y,link}$ and K_{pl} (named in this case b_k) were derived as for the LKH model. All the other parameters, for the isotropic and the kinematic hardening as well, were defined according to usual values provided in literature or finely tuned on the basis of available experimental cyclic tests.

Being E_i the initial hardening ratio, evaluated at the point at which the curve loses linearity and E_{is} the hardening ratio evaluated in the part of the post-elastic branch at which the slope remains constant.

4. Calibration of the link model

The results of the experimental tests were used to calibrate the semi-analytical model proposed. Tested EBFs were modelled using OpenSees (Mazzoni *et al.* 2006); since
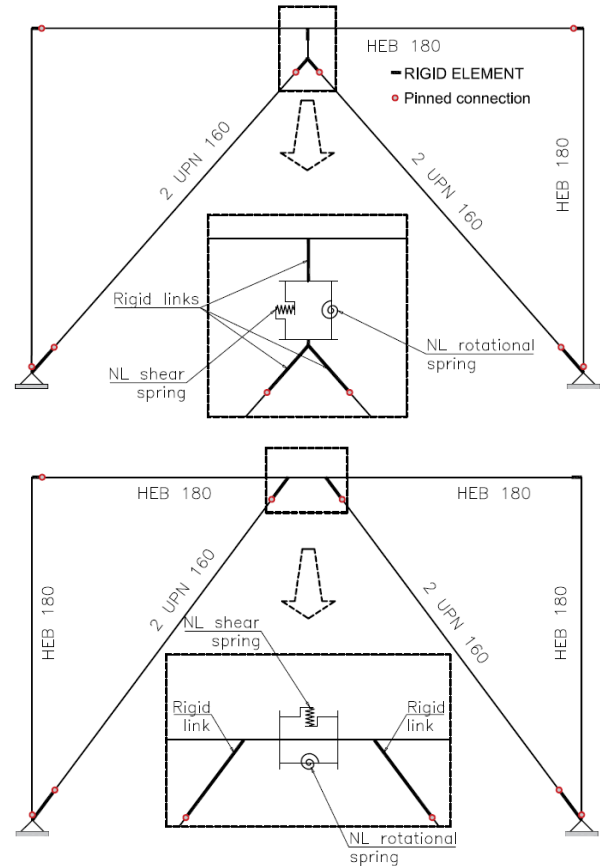

Fig. 18 Numerical models of EBF prototypes

Table 9 Parameters adopted for the numerical modeling

Flexural behaviour (both LKH and NLKH)			
	K_θ [kN/m]	$M_{u,link}$ [kNm]	$M_{y,link}$ [kNm]
Vertical	14666	51.0	61.3
Horizontal	90762	25.0	30.0

Shear behaviour - Linear Kinematic Hardening (LKH)					
		K_y [kN/m]	$V_{y,link}$ [kN]	$V_{u,link}$ [kN]	$D_{u,link}$ [mm]
LKH1	Vert.	476875	145.2	217.8	9.6 (0.08e_{link})
	Hor.	118461	90.1	135.3	24.0 (0.08e_{link})
LKH2	Vert.	476875	145.2	245.0	15.0 (0.125e_{link})
	Hor.	118461	90.2	175.0	37.5 (0.125e_{link})

Shear behaviour - Nonlinear kinematic hardening (NLKH) - both vertical and horizontal links				
Kinematic hardening				
b_k	R_0		r_1	r_2
0.0035	8		0.9	0.25
Isotropic hardening				
b_i	b_l	ρ_i	R_i	L_{vp}
0.00 05	0.005	Ω^*	8	0.0
Ultimate strength				
R_u			f_u	
$V_{y,link}$			8	

Table 10 Experimental vs. numerical results (±110 mrad)

| Vertical link	Exp.	LKH1	LKH2	NLKH
Energy/cycle [J]	8223.3	5881	5579.2	8650.3
Diff. Δ [%]	-	-0.285	-0.322	0.052
Horizontal link	Exp.	LKH1	LKH2	NLKH
Energy/cycle [J]	13250	8748.5	8299.6	12868
Diff. Δ [%]	-	-0.34	-0.374	-0.029

no buckling neither plastic deformations were observed during the tests, columns, beams and braces were modelled by means of linear elastic elements. Connections were modelled considering their 'real' position inside the EBFs with a pinned or a rigid restraint, as represented in Fig. 18. For the dissipative link elements, the semi-analytical model presented in Fig. 15 was used, adopting both LKH and NLKH for the shear/distortion behaviour. In the case of NLKH, the *Steel04* material model (Mazzoni *et al*. 2006) was used.

To assess the limits of LKH and NLKH in the modelling of the *V-γ* relationship of links, a two level comparison, including a first graphic assessment in terms of shape and degradation of the hysteretic capacity and a second evaluation of cumulated energy (global and per cycle), was performed. The erroneous characterization of the hysteretic energy strongly affects the assessment of its seismic capacity.
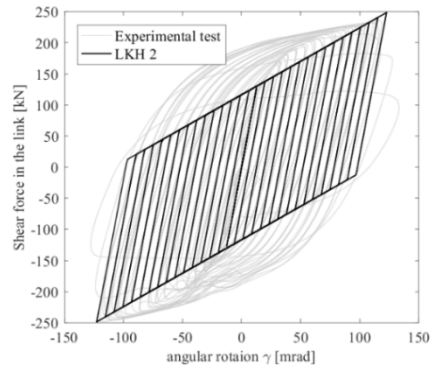
According to the experimental tests and referring to

adopted for the modelling, regarding the flexural and the shear behaviour, valid for the vertical and horizontal link as
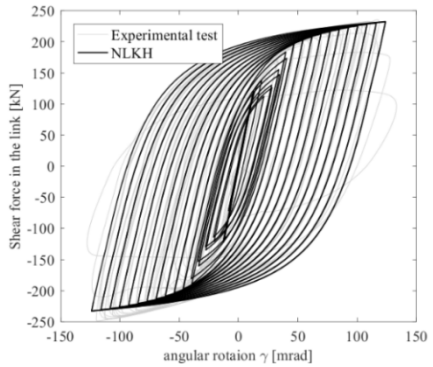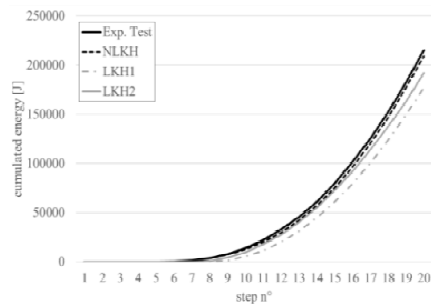
EBF with Horizontal link, ECCS protocol
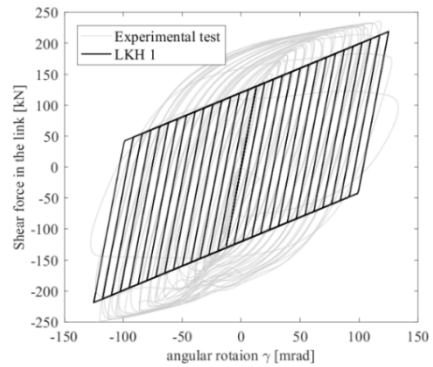
LKH1 vs experimental test

LKH2 vs experimental test

NLKH vs experimental test

Cumulated energy

Fig. 19 Experimental vs numerical cyclic behaviour (horizontal link, ECCS protocol)
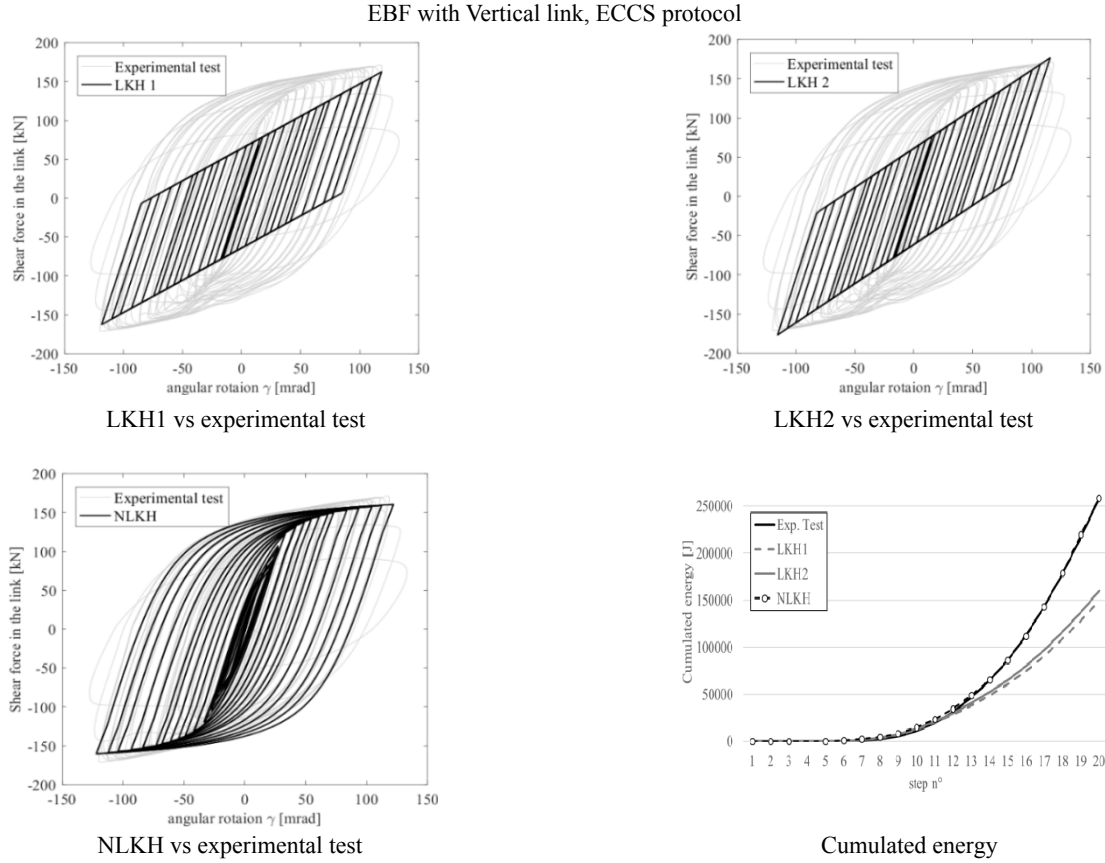
EBF with Vertical link, ECCS protocol

LKH1 vs experimental test

LKH2 vs experimental test

NLKH vs experimental test

Cumulated energy

Fig. 20 Experimental vs numerical cyclic behaviour (vertical link, ECCS protocol)

Vertical link, constant amplitude test
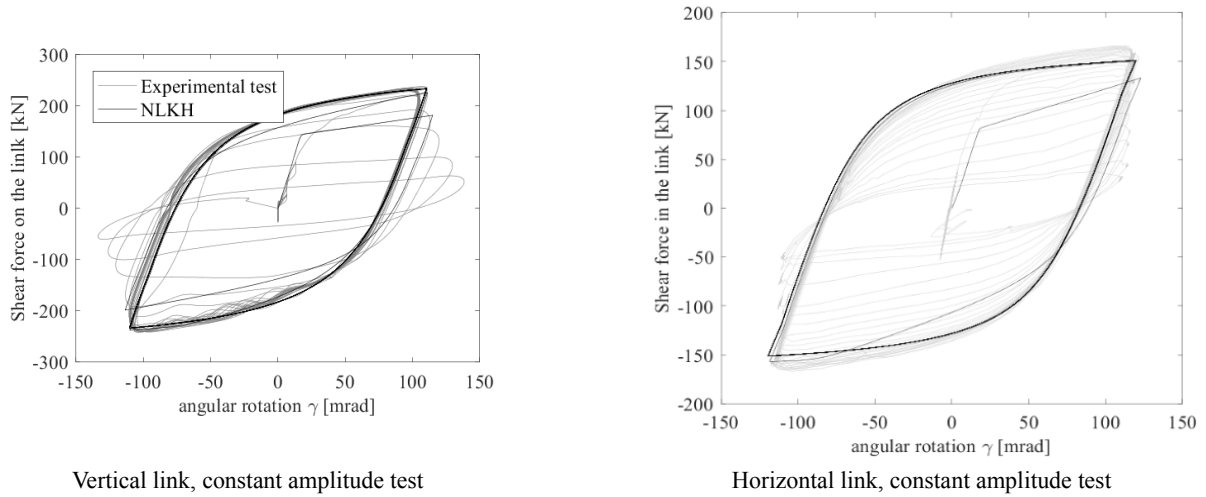

Horizontal link, constant amplitude test

Fig. 21 Experimental vs NLKH numerical cyclic behaviour

what exposed in the previous paragraphs, the values well, are listed in Table 9; the meaning of the adopted parameters is reported in Table 8.

The LKH models, despite its easiness in the calibration process, underestimated the plastic behaviour: the cumulated hysteretic energy coming from the numerical model was always lower than the observed experimental one, with a difference at the collapse (corresponding to an angular distortion of 125 mrad) equal to -22% for the LKH1

and to -10% for the LKH2 (being the negative value related to the underestimation of the cumulated energy).

The experimental tests on the EBFs with horizontal links showed rather high values of the observed Ω_{obs} factor. Evaluating the value for an angular rotation of 80 mrad, the over-strength factor resulted close to 1.90. Furthermore, as just seen for the vertical link, the LKH strongly underestimated the plastic branch, but can correctly matched the collapse behaviour. The cumulated hysteretic

energy was always lower than the one coming from experimental tests.

For the horizontal link, the error in the computation of the cumulated hysteretic energy amounted at -42% and -38% at the collapse, respectively for the LKH1 and LKH2. Such difference was reduced to half, in the case of hysteretic energy computed at 80mrad of angular deformation. Obviously, in both the analysed cases, since the hardening branch of the LKH models was linear, the error in the computation of the cumulated energy was reduced with the increase of the plastic deformations. At 80 mrad, the difference of the results coming from the model with respect to the experimental ones was about -35% and -24%.

As already evidenced for the vertical link, the NLKH model showed a good agreement between the real and the expected cyclic behaviour, reflected on the matching of the cumulated hysteretic energy. Such difference increased at collapse, reaching values close to -43% and -38% (the negative value means an underestimation of the cumulated energy), respectively for the LKH1 and the LKH2 models.

In the case of the constant amplitude, the observations obtained for the LKH1, LKH2 and NLKH models were close to the previously analysed case with the ECCS protocol, for both the vertical and horizontal links. Fig. 21 shows a graphical comparison of the good agreement of the NLKH with the constant amplitude procedure for three models adopted between the numerical and experimental results. The hysteretic energy was again in good agreement with the experimental tests. The absorbed energy per cycle was reported in Fig. 10. As already shown for the ECCS protocol, the discrepancy in terms of absorbed energy between the LKH1 and LKH2 and the experimental tests was apparent.

The comparison between the experimental results and the numerical simulations showed that LKH1, tuned in accordance with the values provided by EN1998-1:2005, notwithstanding the easiness to calibrate it, always underestimated the plastic behaviour of the shear link and, as a consequence, the hysteretic energy. LKH2 and NLKH required the results of experimental for the calibration. LKH2 as well underestimated the plastic behaviour and the hysteretic energy; the differences between the experimental test and the numerical results obtained with the LKH2 were more accentuated for the horizontal link, while in the case of the vertical link, the difference between numerical and experimental results, expressed in terms of cumulated hysteretic energy, was around the 10%. Such difference was not present adopting the NLKH law. Thus, in presence of experimental results, or the knowledge of the effective Ω factor of the link, the adoption of the NLKH is preferable.

5. Conclusions

In the present paper, the results of a wide experimental test campaign executed on EBF real scale one storey/one bay frames equipped with both vertical and horizontal shear links are presented, as well as the elaboration and calibration of a semi-analytical model for the representation of the dissipative behaviour of shear elements.

The execution of cyclic tests, adopting two different loading protocols (i.e., ECCS45 and constant amplitude), allowed to understand the behaviour of dissipative shear links; results of experimental tests, in agreement with what presented in the current scientific literature, highlighted the structural performance of links, with stable behaviour until the initiation of cracks in correspondence of the web and the following degradation of the bearing capacity.

Stating what presented in the current scientific literature concerning the problems related to the link modelling, a simple model consisting of two springs working in parallel representing the flexural (bending/rotation) and the shear (shear/displacement) behaviour has been developed and calibrated using the results of the experimental tests. The model can be employed for the representation of EBF multi-storey buildings without requiring a strong computational effort like the one, for example, associated to the use of solid elements and represent a valid alternative to the models presented in the scientific literature.

Different constitutive laws were adopted for the modelling of the V-γ and M-θ behaviour, based either on a linear kinematic hardening either on a nonlinear kinematic hardening rule. The first relationship was calibrated based on analytical assumptions, while the latter required the results of experimental tests. The analysis of obtained results evidenced that the LKH underestimated the plastic behaviour of the link and, consequently, of the cumulated hysteretic energy. On the other side, the NLKH, able to represent both the isotropic and the non-linear kinematic hardening, properly predicted the plastic branch of the shear link, leading to a satisfactory estimation of the cumulated hysteretic energy.

Simplified approaches, usually adopted in case of statistical analyses requiring a high number of numerical simulations, underestimating the cyclic behaviour of shear links, cannot be then considered reliable enough to be used for the seismic assessment of multi-storey EBF buildings Thus, seen their complex behaviour, the correct estimation of the cyclic behaviour of shear links requires a set of experimental tests trough which calibrate the properties of the NLKH constitutive law.

References

Ashtari, A. and Erfani, S. (2016), "An analytical model for shear links in eccentrically braced frames", *Steel Compos.*

Struct., *Int. J.*, **22**(3), 627-645.

Badalassi, M., Braconi, A., Caprili, S. and Salvatore, W. (2013), "Influence of steel mechanical properties on EBF seismic behaviour", *Bull. Earthq. Eng.*, **11**, 2249-2285.

Badalassi, M., Braconi, A., Caprili, S., Cajot, L.G., Degee, H., Gündel, M., Hjaij, M., Hoffmeister, B., Karamanos, S.A. Salvatore, W. and Somja, H. (2017), "Influence of variability of material mechanical properties on seismic performance of steel and steel–concrete composite structures", *Bull. Earthq. Eng.*, **15**(4), 1559-1607.

Berman, J.W. and Bruneau, M. (2007), "Experimental and analytical investigation of tubular links for eccentrically braced frames", *Eng. Struct.*, **29**(8), 1929-1938.

Berman, J.W. and Bruneau, M. (2008), "Tubular links for eccentrically braced frames. I: Finite element parametric study", *J. Struct. Eng.*, **134**(5), 692-701.

Bertero, V.V., Anderson, J.C. and Krawinkler, H. (1994), *Performance of Steel Building Structures during the Northridge Earthquake*, (Ed. E.E.R. Center), University of California, CA, USA.

Bosco, M. and Rossi, P.P. (2009), "Seismic behaviour of eccentrically braced frames", *Eng. Struct.*, **31**(3), 664-674.

Bosco, M., Marino, E.M. and Rossi, P.P. (2015), "Modelling of steel link beams of short, intermediate or long length", *Eng. Struct.*, **84**, 406-418.

Bouwkamp, J., Vetr, M.G. and Ghamari, A. (2016), "An analytical model for inelastic cyclic response of eccentrically braced frame with vertical shear link (V-EBF)", *Case Studies Struct. Eng.*, **6**, 31-44.

Braconi, A., Caprili, S., Degee, H., Gündel, M., Hjaij, M., Hoffmeister, B., Karamanos, S.A., Rinaldi, V. and Salvatore, W. (2015), "Efficiency of Eurocode 8 design rules for steel and steel-concrete composite structures", *J. Constr. Steel Res.*, **112**, 108-129.

Bruneau, M., Uang, C.M. and Sabelli, S.E.R. (2011), *Ductile Design of Steel Structures*, McGraw-Hill.

D'Aniello, M., Landolfo R, and Della Corte, G. (2012), "Overstrength of Shear Links in Eccentric Braces", *Proceedings of the 15th World Conference on Earthquake Engineering*, Lisbon, Portugal, September.

D.M 14/01/2008 (2008), Norme Tecniche sulle Costruzioni; Ministero delle Infrastrutture, Italia.

Dimakogianni, D., Dougka, G. and Vayas, I. (2015), "Seismic behavior of frames with innovative energy dissipation systems (FUSEIS1-2)", *Eng. Struct.*, **90**, 83-95.

ECCS45, Reccomended testing procedures for assessing the behaviour of structural elements under cyclic loads, in ECCS45; European Convention for constructional steelwork, Technical committee 1, TWG 1.3 – Seismic Design, No. 45.

Engelhardt, M.D. and Popov, E.P. (1989a), "On design of eccentrically braced framess", *Earthq. Spectra*, **5**(3), 495-511.

Engelhardt, M.D. and Popov, E.P. (1989b), "Behavior of long links in eccentrically braced frames", Earthquake Engineering Research Center, Report No. UCB/EERC-89/01; University of California, Berkeley, CA, USA.

Eurocode 8 - EN 1998-1:2005 (2005), Design of Structures for Earthquake Resistance. Part 1: General Rules, Seismic Action and Rules for Buildings; Brussels, Belgium.

FEMA 356 (2000), Prestandard and Commentary for the Seismic Rehabilitation of Buildings; Federal Emergency Management Agency, Washington, D.C., USA.

Gilberson, M. (1969), "Two nonlinear beams with definitions of ductility", *J. Struct. Eng.*, 137-157.

Hjelmstad, K.D. and Lee, S.G. (1989), "Lateral buckling of beams in eccentrically-braced frames", *J. Constr. Steel Res.*, **14**(4), 251-272.

Hjelmstad, K.D. and Popov, E.P. (1983), "Seismic behavior of

active beam links in eccentrically braced fram", Report No. UBC/EERC-83/15; Earthquake Engineering Research Center, University of California, Berkeley, CA, USA.

Kasai, K. and Popov, E.P. (1986), "Cyclic web buckling control for shear link beams", *J. Struct. Eng.*, **112**(3), 505-523.

Keith, D.H. and Egor, P.P. (1983), "Cyclic behavior and design of link beams", *J. Struct. Eng.*, **109**(10), 2387-2403.

Lemaitre, J. and Chaboche, J.L. (1994), *Mechanics of Solid Materials*, Cambridge University Press.

Lian, M., Su, M. and Guo, Y. (2015), "Seismic performance of eccentrically braced frames with high strength steel combination", *Steel Compos. Struct.*, *Int. J.*, **18**(6), 1517-1539.

Lignos, D.G. and Krawinkler, H. (2011), "Deterioration modeling of steel components in support of collapse prediction of steel moment frames under earthquake loading", *J. Struct. Eng.*, **137**(11), 1291-1302.

Manfredi, M., Morelli, F. and Salvatore, W. (2015), "An enhanced component based model for steel links in hybrid structures: Development, calibration and experimental validation", *Proceedings of the 5th ECCOMAS Thematic Conference on Computational Methods in Structural Dynamics and Earthquake Engineering*, Crete Island, June, pp. 3435-3450.

Mastrandrea, L. and Piluso, V. (2009), "Plastic design of eccentrically braced frames, I: Moment–shear interaction", *J. Constr. Steel Res.*, **65**(5), 1007-1014.

Mazzoni, S., McKenna, F., Scott, M.H. and Fenves, G.L. (2006), *OpenSees Command Language Manual*, Pacific Earthquake Engineering Research (PEER) Center.

Mazzolani, F.M., Della Corte, G. and D'Aniello, M. (2009), "Experimental analysis of steel dissipative bracing systems for seismic upgrading", *J. Civil Eng. Manag.*, **15**(1), 7-19.

Mohammadi, R.K. and Sharghi, A.H. (2014), "On the optimum performance-based design of eccentrically braced frames", *Steel Compos. Struct.*, *Int. J.*, **16**(5), 357-374.

Mróz, Z. (1969), "An attempt to describe the behavior of metals under cyclic loads using a more general workhardening model", *Acta Mechanica*, **7**(2), 199-212.

Nakashima, M. (1998), "Classification of damage to steel buildings observed in the 1995 Hyogoken-Nanbu earthquake", *Eng. Struct.*, **20**(4-6), 271-281.

Nakashima, M. and Bruneau, M. (1995), *Preliminary Reconnaissance Report of the 1995 Hyogoken-Nanbu Earthquake*, (Ed. T.A.I.o. Japan).

Okazaki, T. and Engelhardt, M.D. (2007), "Cyclic loading behavior of EBF links constructed of ASTM A992 steel", *J. Constr. Steel Res.*, **63**(6), 751-765.

Peter, D., Ahmad, M.I. and Ian, G.B. (2010), "Cyclic Behavior of Shear Links of Various Grades of Plate Steel", *J. Struct. Eng.*, **136**(4), 370-378.

Popov, E.P. (1983), "Recent research on eccentrically braced frames", *Eng. Struct.*, **5**(1), 3-9.

Prinz, G.S. and Richards, P.W. (2009), "Eccentrically braced frame links with reduced web sections", *J. Constr. Steel Res.*, **65**(10-11), 1971-1978.

Qi, Y., Li, W. and Feng, N. (2017), "Seismic collapse probability of eccentrically braced steel frames", *Steel Compos. Struct.*, *Int. J.*, **24**(1), 37-52.

Ramadan, T. and Ghobarah, A. (1995), "Analytical model for shear-link behavior", *J. Struct. Eng.*, **121**(11), 1574-1580.

Richards, P.W. (2010), "Estimating the stiffness of eccentrically braced frames", *Practice Period. Struct. Des. Constr.*, **15**(1), 91-95.

Richards, P.W. and Uang, C.M. (2005), "Effect of flange width-thickness ratio on eccentrically braced frames link cyclic rotation capacity", *J. Struct. Eng.*, **131**(10), 1546-1552.

Ricles, J.M. and Popov, E.P. (1987), *Dynamic Analysis of Seismically Resistant Eccentrically Braced Frames*, UCB/

EERC-87/07.

Rides, J.M. and Popov, E.P. (1993), "Inelastic link element for EBF seismic analysis", *J. Struct. Eng.*, **120**(2), 441-463.

Roeder, C.W. and Popov, E.P. (1978), "Eccentrically braced steel frames for earthquakes", *J. Struct. Div.*, **104**(3), 391-412.

BU